Semiconducting Polyfluorenes—Towards Reliable Structure–Property Relationships**

By *Ullrich Scherf** and *Emil J. W. List**

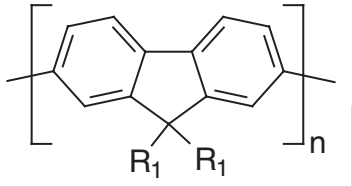

Alkylsubstituted polyfluorenes have emerged as a very attractive class of conjugated polymers, especially for display applications, owing to their pure blue and efficient electroluminescence coupled with a high charge-carrier mobility and good processability. The availability of specific and highly regioselective coupling reactions provides a rich variety of tailored polyfluorene-type polymers and copolymers. The focus of this review, therefore, is on reliable structure–property relationships regarding (i) the interplay of substitution pattern, solid state morphology, and optical/electronic properties, and (ii) the key role of degradation-induced keto defect sites in fluorene-type polymers, and strategies for obtaining defect-free polyfluorenes.

1. Introduction

The electronic properties of many conjugated polymers sensitively depend on their molecular and supramolecular structure. The molecular aspects are often related to the substitution pattern at the conjugated main chain, which determines the conformation of the macromolecule, or to the presence of structural defects. For a maximum π-conjugation along the main chain, the substituents that guarantee the solution processing of the materials should not cause an unwanted distortion of the aromatic building blocks. Regarding this point the 9,9-substituted fluorene moiety represents a very favorable building block for obtaining processable, conjugated polymers, in this case, of the poly(*para*-phenylene)-type (PPP). The unique molecular structure and a couple of other attractive properties (e.g., excellent optical and electronic properties) have brought semiconducting polyfluorenes in the focus of scientific and industrial interest. Moreover, many polyfluorenes show a particular solid-state behavior (regular supramolecular packing, cooperative phenomena such as liquid crystallinity).

The aim of this review is to demonstrate the sensitive interplay between molecular and supramolecular structure as well as the strong influence of the supramolecular structure on the electronic properties within this important class of π-conjugated materials.

2. Polyfluorene Synthesis

First attempts to synthesize soluble, processable poly(2,7-fluorene)s (PFs) via an attachment of solubilizing substituents in 9-position of the fluorene core were published in 1989 by Yoshino and co-workers. They coupled 9,9-dihexylfluorene oxidatively with $FeCl_3$[1] and obtained low molecular weight poly(9,9-dihexylfluorene) (PF6, M_n up to 5000, P_n 9–13). This oxidative coupling is not strictly regioselective, as structural defects are created besides "regular" 2,7-linkages.

The enormous progress in the availability of efficient and strictly regioselective transition metal-catalyzed aryl–aryl-couplings has paved the way for the synthesis of high molecular weight, structurally well-defined PF derivatives. Especially reductive aryl–aryl-couplings of dihaloaryls according to Yamamoto, aryl–aryl cross-couplings of aryldiboronic acids (es-

[*] Prof. U. Scherf
Institut für Chemie, Polymerchemie, Universität Potsdam
Karl-Liebknecht-Str. 24/25, Haus 25, D-14476 Golm (Germany)
E-mail: scherf@rz.uni-potsdam.de
Dr. E. J. W. List[+]
Christian-Doppler Laboratory for Advanced Functional Materials
Institute of Solid State Physics, Graz University of Technology
Petersgasse 16, A-8010 Graz (Austria)
E-mail: e.list@tugraz.at

[+] Second address: Christian-Doppler Laboratory for Advanced Functional Materials, Institute of Nanostructured Materials and Photonics, Franz-Pichler-Strasse 30, A-8160 Weiz, Austria.

[**] Our experiments in the polyfluorene field have been sponsored and supported by SONY International (Europe), Stuttgart (Germany), Stiftung Volkswagenwerk, Hannover (Germany), the Max-Planck-Gesellschaft (Germany), the Sonderforschungsbereich "Elektroaktive Stoffe", TU Graz, Austria, the "Fonds zur Förderung der wissenschaftlichen Forschung—Austria" (P 12806-PHY), and the Christian Doppler Forschungsgesellschaft, Austria. We thank the team of co-workers and collaborators that have been involved in the interdisciplinary research projects on semiconducting polyfluorenes, especially Heinz-Georg Nothofer, Aurelie Falcou, Christopher Schmitt, Roland Güntner, Michael Forster, Patricia Scandiucci de Freitas, Udom Asawapirom, Günther Lieser, Akio Yasuda, Gabi Nelles, Martin Grell, Dieter Neher, Tzenka Miteva, Andreas Meisel, Masao Oda, Dessislava Sainova, Willi Graupner, Alexander F. Pogantsch, Franz P. Wenzl, Andrew C. Grimsdale, Egbert Zojer, Joseph Shinar, and Jean-Luc Brédas. We also thank Klaus Müllen, Wolfgang Knoll, and Günther Leising, for the cooperation as well as their continuous and generous support of our investigations.

  0935-9648/02/0704-0477 $ 17.50+.50/0

ters) and dihaloaryls according to Suzuki, or of distannylaryls and dihaloaryls according to Stille have been successfully applied.

The first transition-metal catalyzed coupling of 2,7-dibromo-9,9-dialkylfluorenes with Ni^{II} salt/zinc was described by Pei and Yang (Uniax Corp.) in 1996.[2] Later on, a research group at DOW Chemical Corp. (Inbasekaran, Woo, and co-workers)[3] as well as Leclerc and co-workers[4] published the synthesis of 9,9-dialkyl-PFs following the Suzuki-type cross-coupling of 9,9-dialkylfluorene-2,7-bisboronic acid or ester and 2,7-dibromo-9,9-dialkylfluorene monomers.

Since the Suzuki-type coupling provides PFs with a maximum M_n of several 10 000, the Yamamoto-type coupling can lead to very high molecular PFs with a M_n of up to 200 000 (P_n: up to 500).[5] The main prerequisite for reaching such high molecular weights is, however, the use of carefully purified monomers and the application of optimized reaction conditions. On the lab scale (up to 10 g batches), the application of $Ni(COD)_2$ as reductive transition metal-based coupling agent is very favorable (Scheme 1).

9,9-Dialkyl-PFs with alkyl side-chains containing more than 6 carbons are highly soluble in various organic solvents. They do not precipitate during the coupling reaction. The length and structure of the alkyl substituents do not significantly vary

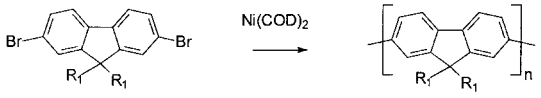

Scheme 1. Synthesis of 9,9-dialkyl-PF according to Yamamoto (R_1: -alkyl).

the optical and electronic properties of the PFs in dilute solution (see Sec. 5), which indicates a negligible influence of the alkyl side-chains on the electronic interaction between adjacent fluorene units. This is a consequence of the very favorable 9-position of alkyl-substitution in 9,9-dialkyl-PFs, which is far away from the aryl–aryl-coupled 2- and 7-positions. However, the structure of the alkyl side-chains strongly influences the solid-state packing of the polymers; especially *n*-alkyl derivatives display a unique aggregation behavior in the condensed phase (β-phase formation; see Sec. 3 and 5.1). This special solid-state packing can be suppressed in branched alkyl chain-substituted PF derivatives, i.e., their solid-state properties do not differ significantly from their single molecule (solution) properties. Increasing the alkyl chain length, the T_g-value is reduced gradually, poly[(9,9-bis(3,7,11-trimethyldodecyl)-fluorene)-2,7-diyl], for example, is very soft at ambient conditions and shows a T_g below room temperature.[6]

Routine size exclusion chromatography (SEC) measurements of PFs (polystyrene, PS, calibration) display overestimated numbers of M_n and M_w due to the rigid-rod or, better, semirigid-rod nature of the polymers. Dynamic light scattering experiments on narrowly distributed poly[(9,9-bis(2-ethylhexyl)fluorene)-2,7-diyl] (PF2/6) fractions, which have been prepared by preparative SEC fractionation, have displayed reduced absolute M_w values (50–70 %) in relation to the PS-calibrated SEC results.[7] Based on small-angle-neutron scattering and translational diffusion measurements in dilute solutions, the polymer chains can be described as wormlike chains with a relatively low persistence length L of ca. 7 nm. This reflects the

Prof. Ullrich Scherf studied chemistry at the Friedrich-Schiller University of Jena, Germany and obtained his Diploma (MSc.) in 1983, and his Ph.D. in 1988. He joined the Max-Planck Institute for Polymer Research in Mainz in 1990. He received his Habilitation in 1996. He won the Meyer-Struckmann Research Award in 1998 and became Professor for Polymer Chemistry at the University of Potsdam, Germany, in 2000. His research interests include the synthesis of novel and unique polymeric architectures that are applicable as active components in electronic devices (light-emitting diodes, field-effect transistors, photovoltaic cells, photodiodes, and polymer lasers).

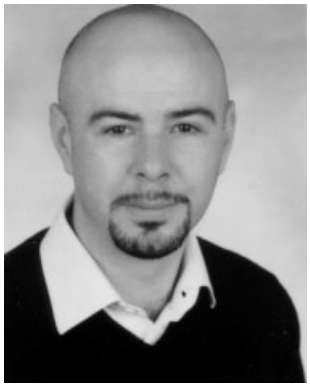

Dr. Emil List graduated from the Graz University of Technology, Austria, in 1998 as a Diplom-Ingenieur (MEng). After his Master's degree he went on to do a Ph.D., which he obtained in 2000 from the Graz University of Technology. He then started a post-doctoral position working on FWF and SFB projects, and in 2001 he moved to the Institute of Solid-State Physics at his home university. On January 1, 2002, he became Head of the Christian-Doppler Laboratory for Advanced Functional Materials. His main research interests are focussed on fundamental physics (optical spectroscopy and spectroscopy on devices) and electronic device applications of organic semiconductors (conjugated polymers as well as advanced functional organic and inorganic materials).

0935-9648/02/0704-0478 $ 17.50+.50/0

ADVANCED MATERIALS

semirigid nature of the chains, a result of the kinked and distorted arrangement of the fluorene structural units.

The structure of the PF homopolymers can be varied by co-condensation with suitable comonomers. The use of monofunctional comonomers leads to an attachment of defined end-groups (so-called end-cappers, Scheme 2). In this way, additional chemically, chromophorically, or electronically active

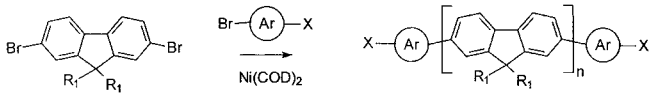

Scheme 2. Synthesis of terminally end-functionalized 9,9-dialkyl-PF (R_1: -alkyl, X: -CH=CH_2, -NPh_2, -NH_2, ...).

functional groups can be introduced into the terminal positions of the PF backbones. Examples for this strategy are styryl-end-capped, crosslinkable PFs,[8] triarylamine-(e.g., triphenylamine TPA)-end-capped derivatives with improved hole-transporting properties for use in organic light-emitting diodes (OLEDs),[9] PFs with terminal dendronic units,[10] or aniline-end-capped PFs as intermediates for the design of novel conjugated/conjugated block copolymers.[11] The use of difunctional comonomers opens the way for several fluorene-based copolymers. Following the Yamamoto-type coupling, statistical copolymers are accessible, which contain, e.g., anthracene, perylene, carbazole, cyclopentadithiophene, or other arylene building blocks (Scheme 3).[12] Applying the cross-coupling methods according to Suzuki or Stille a bundle of alternating copolymers can be synthesized, e.g., alternating fluorene/thiophene, fluorene/bithiophene, fluorene/triphenylamine copolymers (Scheme 4).[13] A couple of these copolymer structures is listed in the patents held by DOW Chemical Corp.[3]

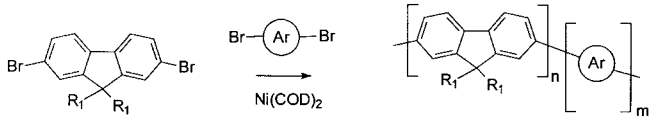

Scheme 3. Synthesis of statistical PF/polyarylene copolymers (R_1: -alkyl, Ar: 9,10-anthrylene, (4,4-dialkyl)-4H-cyclopenta[2,1-b:3,4-b′]dithiophene-2,6-diyl, *N*-alkylcarbazole-3,6-diyl, etc.; X: -$B(OH)_2$, -$B(OR)_2$, -SnR_3).

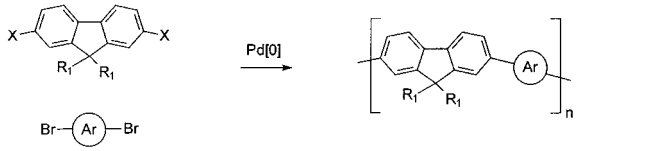

Scheme 4. Synthesis of alternating fluorene-2,7-diyl/arylene copolymers (R_1: -alkyl, Ar: *N,N,N*-bis(phenyl-4-yl)-(4-methylphenyl)amine, 2,5-thienylene, 2,2′-bithienyl, etc.).

As mentioned before, PFs containing aniline end-functions can be used for the preparation of novel polyaniline/polyfluorene/polyaniline ABA-type triblock copolymers as described by Scherf and co-workers (Scheme 5).[11] The PANi/PF/PANi block copolymers contain two electronically active conjugated blocks of rather different redox properties, which are, in combination with the observed nanoscale phase-separation, attractive for the design of organic solar cells. An AFM image of such a PANi/PF/PANi block copolymer (Fig. 1) illustrates the formation of phase-separated morphologies on the nanoscale.

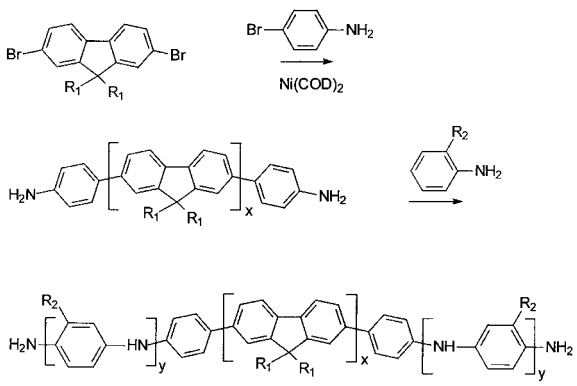

Scheme 5. Synthesis of conjugated PAni/PF/PAni triblock copolymers (R_1, R_2: -alkyl).

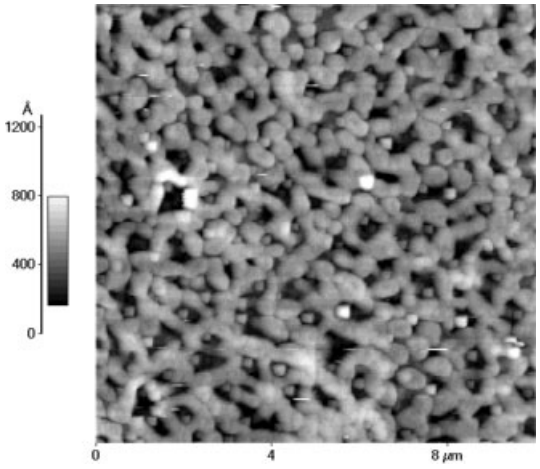

Fig. 1. AFM image of a PANi/PF/PANi triblock copolymer (ABA-type) spin-coated film on an untreated glass substrate.

An important point concerning the application of PF-based materials in electronic devices (LEDs, solid-state lasers, solar cells) is related to the presence (or absence!) of defect states. A study of List, Scherf, and co-workers has outlined possible ways of defect state generation in PFs[6] (see Sec. 5.2). One crucial point for avoiding defects is the use of completely 9,9-difunctionalized fluorene monomers. The presence of small amounts of non-alkylated or only monofunctionalized monomers (9-alkylfluorene derivatives) yields preferred centers for oxidative/photooxidative degradation. Such centers can be already oxidized during the coupling reaction/atmospheric work-up under formation of fluorenone structural units. They can act as quenching sites for optical excitations or charges (energy or charge traps). The complete absence of benzylic hydrogens in the 9-position of the fluorene moiety seems to be a key prerequisite for obtaining oxidatively stable, defect-poor PFs. Besides this, the overall purity of the difunctional monomers is crucial for reaching high molecular weights, especially in the aryl–aryl coupling according to Yamamoto.

  0935-9648/02/0704-0479 $ 17.50+.50/0

3. Solid-State Ordering and Morphology

As mentioned in the section before, the structure of the alkyl side-chains in the 9-position of the fluorene moieties strongly influences the solid-state packing of the polymers. *n*-Alkyl derivatives display a unique packing behavior in the condensed phase upon thermal treatment,[14] upon exposing the films to solvent vapors,[15] or treating the polymer with solvent/non-solvent mixtures of increasing non-solvent content.[16] For such samples, in addition to the regular, glassy (α) phase, a novel, so-called β-phase, has been identified. Compared to the glassy phase of PF, the β-phase shows a distinct red shift of absorption and emission peaks with a remarkably well-resolved vibronic progression both in absorption and emission (see Sec. 5.1). In contrast, the glassy phase of PF only reveals a well-resolved vibronic progression in the emission spectrum. A comparison to PPP-type polymers with a fully planarized backbone (ladder-type PPP or LPPP, see Scheme 6) shows very similar absorption and emission characteristics for β-phase PF and LPPP, which leads to the conclusion that the initially distorted backbone of PF is flattened into a planarized conformation during β-phase formation. Note that PF, in contrast to LPPP, possesses torsional freedom between adjacent fluorene units. The resulting more extended **intra**chain π-conjugation accounts for the observed bathochromic shift and the well-resolved vibronic progression in the absorption and emission of β-phase-PF (as discussed in detail in Sec. 5.1). No evidence for distinct **inter**chain interactions of the π-electron systems of the PF chains was observed (ground state aggregate or excimer formation). Hence the driving force for this unique packing behavior (β-phase formation) has to be attributed to a solid-state packing, e.g., of the *n*-alkyl side-chains (so-called side-chain crystallization), described as "mechanical stress during β-phase formation".[17] This is in full agreement with the observation that this special solid-state packing is fully suppressed in the case of branched alkyl chain-substituted PF derivatives (especially with 2-ethylhexyl, 3,7-dimethyloctyl, or most favorably, 3,7,11-trimethyldodecyl side chains).[6] Then, the solid-state optical properties of this PF derivatives do not differ significantly from their single molecule (dilute solution) properties, besides slight bathochromic shifts of the solid-state absorption and emission peaks. Such a behavior was also described for dendron-substituted PFs, at the same time and independently by Müllen and co-workers,[17] and Carter and co-workers.[18]

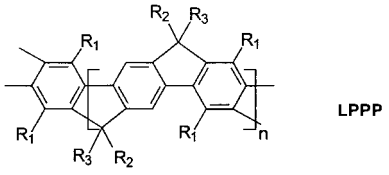

Scheme 6. Structure of planarized PPP-type ladder polymers (LPPP, R_1: -alkyl, R_2: -aryl, R_3: -methyl, -phenyl, or -H).

X-ray and electron diffraction measurements support this interpretation. For 9,9-di-*n*-octyl-PF (PF8, or PFO) it was found that the correlation length in chain direction, a measure of the **intra**chain order of a polymer, is much longer (22 nm) for the β-phase-PF relative to the glassy (α) phase (ca. 8.5 nm) according to X-ray fiber diffraction measurements.[19] Since the correlation length of the glassy (α) phase of PF8-fibers equals that in solution (and also matches the so-called effective conjugation length) one can conclude that a more effective (extended) conjugation occurs in the β-phase due to the already mentioned backbone planarization. In contrast, Lieser and co-workers have investigated thin films and fibers of a PF with branched side-groups, poly[(9,9-bis(2-ethylhexyl)fluorene)-2,7-diyl] (PF2/6), by X-ray and electron diffraction measurements.[20] They found the complete absence of the β-phase in PF2/6 (Fig. 2). The distorted (α-phase) PF chains display a regular hexagonal packing. Very remarkably, single PF chains show a helical conformation (5_1 or 5_2 helix). The extended conjugation within the chains, however, rules out a 5_1 helix. A 5_2 helix corresponds to a 36° distortion between adjacent fluorene moieties. This finding leads to the question whether control of the helical sense is possible via introduction of chiral alkyl substituents in the 9-position of the fluorene core (a review on chiral conjugated polymers has been published previously[21]). The successful execution of such a strategy was presented recently.[26]

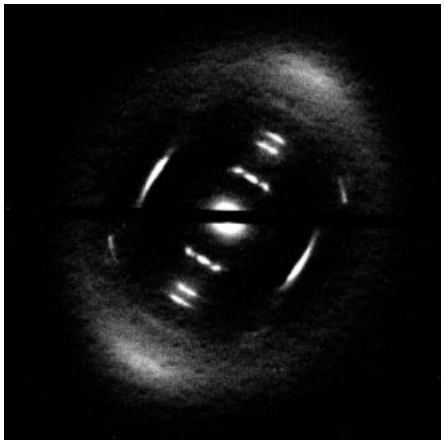

Fig. 2. Electron diffraction pattern of a highly oriented di(2-ethylhexyl)-PF-(PF2/6) film (thickness ca. 40 nm, oriented at 200° on rubbing-aligned polyimide, circular area of 2.7 μm diameter with the meridian in direction SW-NE).

Additional insight into the solid-state arrangement of β-phase-forming 9,9-di-*n*-hexyl-PF (PF6) came from NSOM fluorescence microscopy investigations by Vanden Bout and co-workers.[22] Their results indicate that annealed (and/or aligned) samples of 9,9-di-*n*-hexyl-PF possess a richer morphology than previously believed. They observed highly ordered ribbonlike (microcrystalline) features with nanometer dimensions (40–70 nm × 500–1000 nm).

4. Liquid Crystallinity

Many 9,9-dialkyl-PFs display a very unique phase behavior; they can form thermotropic LC mesophases as first shown by

  0935-9648/02/0704-0480 $ 17.50+.50/0

ADVANCED MATERIALS

Bradley and co-workers.[23] The melting into a birefringent fluid phase—(partially) crystalline state → LC state—was found to be in the temperature range of 100–180 °C for several PFs with linear and branched alkyl substituents (6–15 carbon atoms) in the 9-position of the fluorene moiety. Di-*n*-octyl-PF, e.g., shows a T_{Cr-LC} phase transition at ca. 160 °C; di(2-ethylhexyl)-PF (see Fig. 3, Table 1) exhibits this transition at ca. 167 °C. Other branched alkyl chain-substituted PFs (e.g., di(3,7-dimethyloctyl)-PF and di(3,7,11-trimethyldodecyl)-PF) are not crystalline; according to differential scanning calorimetry (DSC) and X-ray diffraction, their frozen LC states soften at lower temperatures (T_g at ca. 100 °C for di(3,7-dimethyloctyl)-PF, or at ca. 68 °C for di(3,7,11-trimethyldodecyl)-PF).

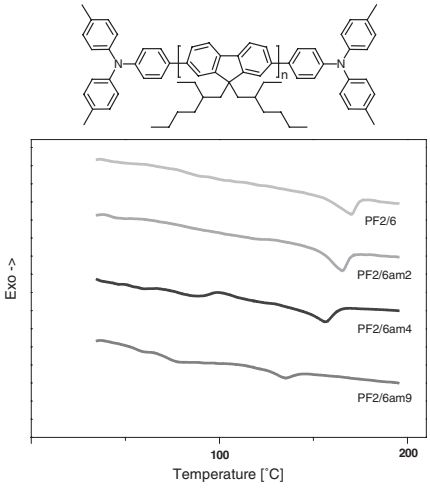

Fig. 3. Molecular weight control and transition-temperature tuning in TPA-end-capped di(2-ethylhexyl)-PF (PF2/6 amX).

Table 1. Data for molecular weight control and transition-temperature tuning in PF2/6 amX (Fig. 3).

	M_n [g mol^{-1}]	M_w/M_n	End-capper concentration [%] [a]	T_{LC} [°C]
PF2/6	122 000	2	0	169
PF2/6 am2	102 000	1.42	1.4	163
PF2/6 am4	48 400	1.55	3.0	152
PF2/6 am6	12 000	2.57	8.3	135

[a] Data obtained from NMR measurements.

The transition temperatures are, of course, molecular weight dependent as shown in Figure 3 for a series of (partially crystalline) TPA-end-capped PF2/6amX derivatives. The transition temperatures in alternating di-*n*-octylfluorene/bithiophene copolymers, which are attractive for a potential use as semiconducting layers in organic field-effect transistors (OFETs), are increased by more then 100°C (275–285 °C) in relation to the corresponding PF homopolymer (PF8) as a consequence of incorporation of the rigid, unsubstituted bithiophene moieties.[24]

The LC mesophases of dialkyl-PFs were characterized as nematic.[25] Higher ordered LC mesophases have been, however, observed for monoalkyl-PFs (sandinic mesophases). Chiral alkyl chain-substituted PFs can form chiral LC mesophases.[26] The clearing point (transition in the isotropic state) is located at rather high temperatures of >250 °C, and is often not detectable, since decomposition has already started.

Because of their unique phase behavior, PF-films are very promising candidates for orientation experiments in order to achieve a monodomain alignment with high dichroic ratios of absorption, or with a highly polarized photo- (PL) or electroluminescence (EL). In terms of absorption and photoluminescence this has been first demonstrated for di-*n*-octyl-PF, which was oriented on rubbed polyimide orientation layers (dichroic ratio in absorption: 6.5; polarization of PL: 10).[23,27] However, the use of branched alkyl chain-derivatives leads to an improved monodomain alignment (dichroic ratio in absorption: 15; polarization of PL: 18).[28] An alternative orientation on organic photoalignment layers (based on the isomerization of diazo groups; so-called PAPs) is also possible.[29]

The first organic light-emitting diodes (OLEDs) that emit polarized blue light (polarization of EL up to 30) have been described by Neher, Scherf, and co-workers.[28]

TEM images of thin, aligned PF2/6-films have, however, shown that monodomains are not really formed. The aligned films display a lamellar morphology and are composed of highly oriented stripes with regions of lower orientation in between them (Fig. 4).[20]

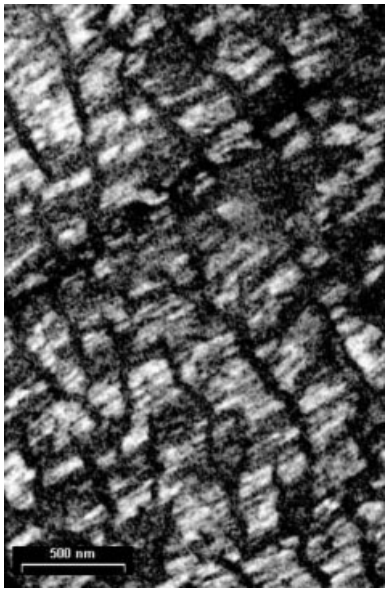

Fig. 4. TEM images of the thin, aligned PF2/6 layer from Figure 2 (dark field image in the light of the 00.5 reflection); the light regions represent highly oriented, lamellar PF2/6 domains (diameter: 50–300 nm), the dark regions are domain boundaries that are filled with non-aligned material.

5. Optical and Electronic Properties

Polyfluorenes display a rich and attractive variety of optical and electronic properties. In the following we will focus on properties that are related to the above mentioned **intra**chain order effects of the polymer backbone (β-phase formation) as well as on those that are related to an ongoing (oxidative)

  0935-9648/02/0704-0481 $ 17.50+.50/0

degradation of the material. The latter is of special importance, since PFs have emerged as the most promising class of active, emissive materials for deep-blue OLEDs.

5.1. Morphology-Related Optical Properties

Polyfluorenes in dilute solution display an unstructured long-wavelength absorption maximum λ_{max} centered at ca. 380 nm (3.25 eV), nearly independent from the substitution at the 9-position as depicted in Figure 5. In photoluminescence, polyfluorenes typically display a vibronically well-resolved emission spectrum with an energetic spacing of ca. 180 meV (related to the stretching mode of C=C–C=C substructures of the polymer backbone) with the 0–0 electronic transition centered at ca. 2.9 eV.

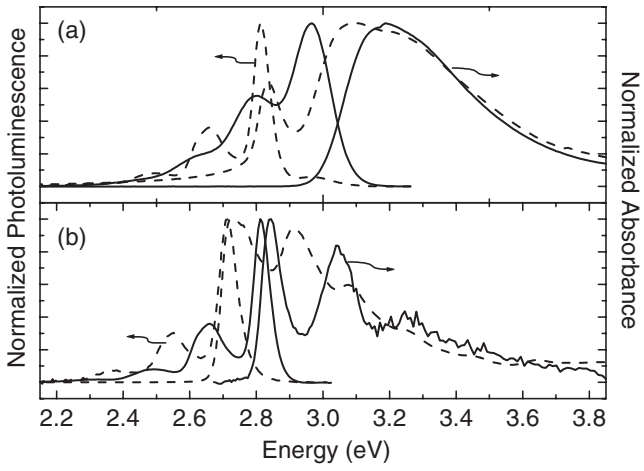

Fig. 5. a) Absorption and photoluminescence spectra of PF8 in dilute solution (chloroform, solid lines) and after partial agglomeration (β-phase formation) in a chloroform/methanol mixture (v/v, 75:25, dashed lines); b) Absorption and photoluminescence spectra of the so-called β-phase of polyfluorene (solid lines, as derived from a numerical subtraction of the absorption and emission spectra in chloroform and in chloroform/methanol mixture, 75:25). For comparison the absorption and photoluminescence spectra of LPPP (R_1: -hexyl, R_2: -4-decylphenyl, R_3: -methyl) is given (dilute solution, toluene, dashed lines).

As already mentioned in Section 3, *n*-alkyl-PFs can undergo a conformational change during transition in the condensed state. The formation of a second phase, the β-phase, was observed under certain experimental conditions (see Sec. 3). Essentially, this effect was recently also observed for poly-(9,9-dioctylfuorene) (PF8) in solvent/non-solvent mixtures (chloroform/methanol) of increasing non-solvent content, which gives rise to an agglomeration of individual polymer chains (Fig. 5a).[16] The agglomeration (particle formation) is detectable, e.g., by light scattering and microfiltration. In the case of PF8, the agglomeration of single macromolecules is accompanied by the occurrence of a series of novel, red-shifted absorption peaks at ca. 2.85 eV, 3.04 eV, and 3.22 eV, as an indication of the β-phase formation (Fig. 5b). The relative intensity of the new β-phase-related bands increases for increasing non-solvent content, and simultaneously the intensity of the broad unstructured PF absorption decreases.

The PL spectrum of di-*n*-octyl-PF (PF8) in chloroform/methanol mixtures also dramatically changes with increasing non-solvent content. Novel features at lower energies (2.81 eV, 2.65 eV, and 2.49 eV) arise, in addition to the still observed emission bands of "isolated" (molecularly dissolved) PF chains, which are, however, diminished at higher methanol contents.

A clearer picture can be derived from the difference spectra of partly agglomerated (β-phase) and "isolated" PF chains both in absorption and emission (as shown in Fig. 5b). These findings are very similar to results obtained for thermally cycled PF8-films.[15]

The newly emerging red-shifted absorption and emission features of PF8 possess, in contrast to "isolated" PF chains, a vibronic progression both in absorption and emission, which is characteristic for a chain geometry with an extended π-conjugation.

As a result of the agglomeration, the *n*-alkyl side-chains force a unique packing of the polymer chains with a more coplanar arrangement of the fluorene building blocks and an increased π-conjugation along the polyfluorene main chain.

When comparing the absorption and emission spectra of β-phase-PF and fully planarized PPP-type ladder polymers LPPP a first observation is that both materials possess nearly identical spectral characteristics (Fig. 5b). The only difference is a slight red-shift of ca. 100 meV for the absorption and emission spectra of LPPP. β-Phase PF and LPPP display an identical vibronic progression. The observed vibronic fine-structure of β-phase PF in the absorption spectrum is fully consistent with our interpretation of a side-chain driven planarization of the PF backbone. LPPP and β-phase PF show a similar geometrical main-chain arrangement, and, hence, similar ground- and excited-state parabola of the energy levels. In contrast, the absence of a well-resolved vibronic structure in the absorption of "isolated" PF chains is indicative of a distinct geometry change during transition from the ground state to the excited state, which is documented by rather differently shaped ground- and excited-state energy parabolas, as also observed, e.g., for biphenyl.[30]

In addition to the remarkable similarities between the absorption and emission spectra of LPPP and β-phase-PF, a comparable similarity is found for photoinduced spectral features, such as triplet excitons[14,31] and polarons, which occur at nearly identical energies for both β-phase-PF and LPPP (P1 @ 0.5 eV[14] and P2 @ 1.9 eV.[14,31] (For the definition of the triplet and polaronic states, see the inset of Fig. 6). It was also shown that in films composed of both "regular" (α-phase) and β-phase PF a dramatic increase in the polaron steady state density occurs as a consequence of the increase of the energetic disorder in the bulk material.[31] Since a high steady state polaron density represents a serious drawback in OLED and solid-state laser applications, due to non-radiative quenching of singlet excitons at trapped polarons, PF derivatives without β-phase formation (branched alkyl side-chains in 9-position) have to be favored.[32]

0935-9648/02/0704-0482 $ 17.50+.50/0

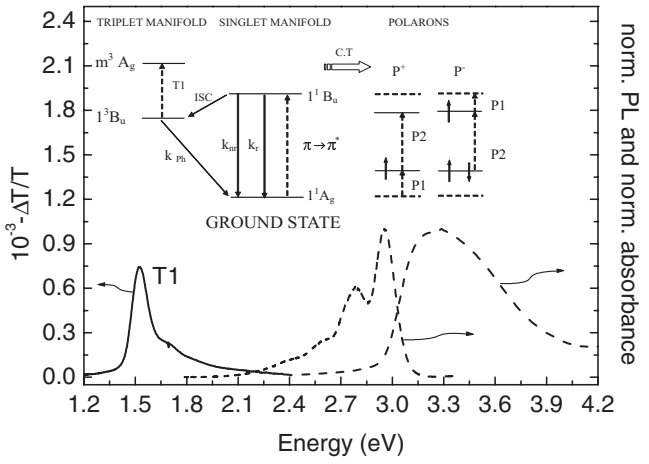

Fig. 6. Absorption (dashed line), photoluminescence (PL, dotted line), and photoinduced absorption (PA, solid line) spectra of a PF2/6 film. The inset shows the schematic Jablonski diagram for this PF-material; depicted are the energy levels and optical transitions associated with singlet, triplet, and charged excitations. The 1^1A_g and the 1^3B_u states are the ground state and lowest triplet exciton (TE) states, respectively. The 1^1B_u is the lowest allowed excited singlet exciton (SE) state. k_r and k_{nr} are the radiative and non-radiative rate constants for the 1^1B_u singlet exciton (SE) decay. T1 denotes the first allowed triplet absorption from the 1^3B_u to the lowest excited m^3A_g state as observed in photoinduced absorption (PA), while k_{PH} is the radiative phosphorescent decay of triplets to the ground state. P^+ and P^- represent polarons created upon charge transfer (CT), while P1 and P2 are the optical transitions within the polaronic states.

Despite the rich physics contained in the solid-state packing of di-*n*-alkyl-PFs (e.g., PF8) we will now focus on the optical and electronic properties of branched alkyl chain-substituted PF derivatives that show a suppressed β-phase formation.[6,16,28]

PFs with branched alkyl chain substituents typically display a solid-state emission spectrum that is nearly identical to the spectra in dilute solution, only a very slight bathochromic shift of ca. 100 meV is observed. The absorption band in the solid state is slightly broadened as a result of small local variations of the π-overlap due to some conformational disorder.[31]

As shown in Figure 6 the photoinduced absorption (PA) of the branched alkyl chain-substituted PF derivative PF2/6 shows one dominant band peaking at 1.54 eV. This band is assigned to a transition from the 1^3B_u to a higher lying m^3A_g triplet state (T1 absorption), similar to the PA of methyl-substituted ladder-type PPP (MeLPPP).[31]

From pulsed radiolysis measurements the energetic spacing between the ground state 1^1A_g and the lowest triplet exciton state 1^3Bu has been found to be 2.1 eV.[33d] This is in excellent agreement with the observed phosphorescence energy of PF2/6 at ca. 2.1 eV.[33] It is worth noting that PF2/6 exhibits exceptionally high solid-state PL quantum yields, which have been found to be on the order of 50–60 %. Typical radiative PL decay times were measured to be in the region of ca. 1 ns.[25,34]

Remarkably, PF2/6 films do not exhibit a significant polaronic absorption band in steady-state PA measurements (see Fig. 6) as a consequence of the rather low density of traps and low energetic disorder of the bulk polymer, which are both needed to create and stabilize polarons.[31]

The low concentration of polaronic species and the small overlap of the PA with the PL emission make PF2/6 and related derivatives promising candidates for organic solid-state lasers since the absence of a PA/PL overlap is a required feature for this type of application.[35,36] The low energetic disorder is also reflected in the rather high charge carrier mobility of polyfluorenes of up to 3×10^{-4} cm^2/Vs (for holes) combined with the observation of a non-dispersive charge carrier transport from TOF measurements.[37]

5.2. Degradation-Related Optical and Electronic Properties

Aside from the above discussed morphology-induced changes (β-phase formation) and their impact on the materials science of PF-type polymers the observation of distinct photophysical changes due to photo- and/or electro-degradation processes is of outstanding importance for device applications. Yet, despite the remarkable improvements in terms of stability and color purity of OLEDs based on PF-type emitters, most of these OLEDs suffer from a degradation of the device under operation, which is most visibly documented in the formation of a low energy emission band at 2.2–2.3 eV. This behavior turns the desired blue emission color into an undesired blue–green emission. This band, which is also found in photoluminescence (PL) after photooxidation of the polymer, has been mostly attributed to aggregate and/or excimer formation in the material.[38,39]

However, as shown recently[6] the more or less intense low-energy emission band at 2.2–2.3 eV can be identified as the emission from exciton and/or charge trapping keto defect sites (9-fluorenone sites), which in fact can be regarded as emission of a guest (defect) accidentally incorporated into the π-conjugated PF backbone. As shown below, such keto defects, leading to the unwanted low energy emission band in polyfluorenes, can be formed already during synthesis (in the case of 9-monoalkylated polyfluorenes, MA-PF), or as result of a photo- (or electro-) oxidative degradation process of almost any PFs, now shown for a 9,9-dialkylated polyfluorene (DA-PF).

The 9-monoalkylated polyfluorene MA-PF and the 9,9-dialkylated derivative DA-PF discussed here (alkyl = 3,7,11-trimethyldodecyl) can be synthesized from the corresponding 2,7-dibromofluorene monomers in a reductive aryl–aryl coupling according to Yamamoto (see Sec. 2). The long and branched (3,7,11-trimethyldodecyl)-side-groups hereby allow a simple liquid chromatographic separation of mono- and dialkylated dibromofluorene monomers to be carried out, which is more difficult for PFs bearing smaller side-chains. We found that pristine 9-monoalkylated MA-PF already contains 9-fluorenone defect sites after polymer synthesis. An explanation for the ongoing mechanism of defect-site generation is the following (see Scheme 7): The highly active Ni^0 species used in the reductive coupling of the dibromo monomers reduce a certain amount of the 9-monoalkylated fluorene building blocks (I) to (aromatic) fluorenyl anions (II) under forma-

  0935-9648/02/0704-0483 $ 17.50+.50/0

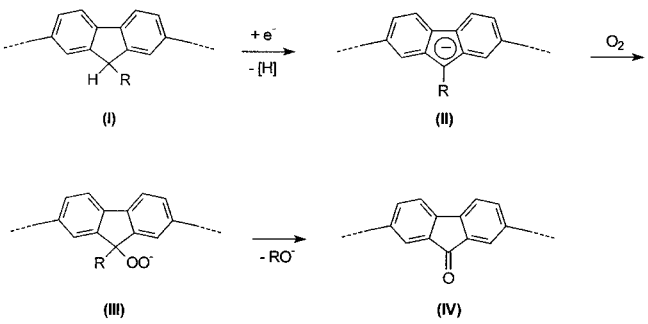

Scheme 7. Proposed mechanism for the generation of keto defect sites in MA-PF (for explanations see Sec. 5.2).

tion of hydrogen. These anions can form hydroperoxide anions (III) with atmospheric oxygen during the work-up of the reaction mixture. The hydroperoxide anions then undergo a final rearrangement to fluorenone moieties (IV).

The incorporation of the fluorenone defect sites in MA-PF dramatically changes the emission properties of the polymer; for a comparison of the PL spectra of MA-PF and defect free 9,9-dialkyl-PFs see Figures 5a, 6, and 7a.

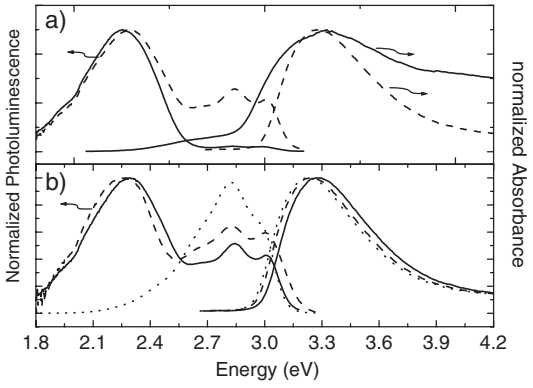

Fig. 7. a) Absorption and photoluminescence emission of MA-PF in dilute solution (cyclohexane, dashed line) and in the solid state (full line). b) Absorption and photoluminescence emission of MA-PF in different solvents: cyclohexane (full line), toluene (dashed line), and dichloromethane (dotted line).

MA-PF in dilute solution exhibits a broad absorption peak at 3.2 eV and a PL emission spectrum showing maxima at 2.95 eV and 2.8 eV as well as an unexpected low energy band peaking at 2.3 eV. In the solid state the absorption of MA-PF becomes much broader and an additional weak contribution centered at ca. 2.8 eV occurs. In contrast to the emission spectrum of MA-PF in dilute solution (toluene), the solid-state PL spectrum is dominated by the low-energy emission peak at ca. 2.28 eV.

Contrary to MA-PF, DA-PF exhibits very similar absorption and emission spectra both in toluene solution and in the solid state; moreover, these spectra are almost identical to the spectral features of PF2/6 as shown in Figure 6. Both the PL emission spectrum of DA-PF in dilute solution and in the solid state show a complete absence of the lower energy contribution at ca. 2.3 eV.

Comparing the energetic position of the π^*–π transition at 2.9 eV and its vibronic replica in the PL spectrum of DA-PF with the two emission peaks of MA-PF at 2.95 eV and 2.8 eV, these transitions are assigned to emission from the delocalized π-electron system of regular, defect-free polyfluorene chains. In contrast, the low-energy emission band at 2.3 eV, which is only found in MA-PF, has a different origin that is not related to the emission from the undisturbed, defect-free PF backbone. From a comparison with literature results, this emission band is assigned to stem from keto defect sites, namely fluorenone building blocks, which have been found to emit exactly at this energetic position.[40]

The observed solvatochromism of the low-energy emission band at ca. 2.3 eV supports the assignment to fluorenone building blocks and reflects the considerable permanent dipole moment of the >C=O moiety (see Fig. 7b). For MA-PF dissolved in dichloromethane the fluorenone emission band is completely absent. The more polar solvent molecules are more closely bound to the excited state fluorenone building blocks, this favors non-radiative deactivation processes ("solvent quenching"). It should be noted that the observed effect is not concentration-dependent, which is an additional argument against aggregation and/or excimer formation as the origin of the emission band at 2.3 eV.

The assignment of the low-energy emission band to the presence of yellow/orange emitting fluorenone defect sites is in agreement with the observation of an additional IR band at ca. 1721 cm^{-1} in pristine MA-PF samples as shown in Figure 8a. This signal is not detectable in pristine DA-PF as depicted in the same figure. This band has been identified as the carbonyl stretching mode (>C=O) of the fluorenone building block.[41] Furthermore the weak low energy tail of the MA-PF

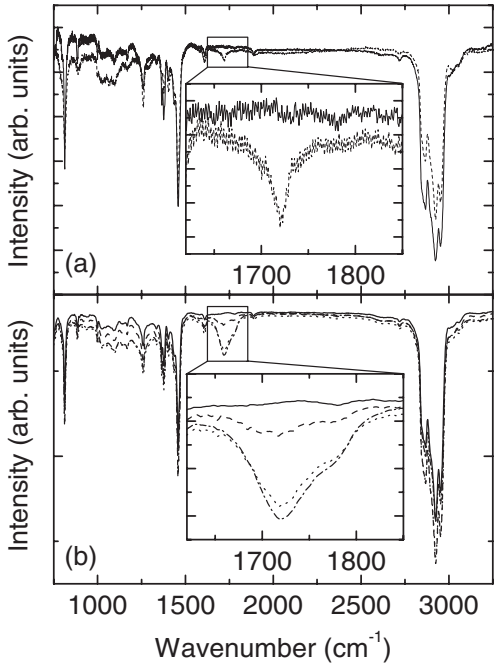

Fig. 8. IR transmission spectra of MA- and DA-PF films on Si: a) MA-PF (dashed line) and DA-PF (full line). b) "Pristine" DA-PF (full line), and this film after photooxidation (1000 W xenon lamp under air) for 2 (dashed line), 4 (dotted line), and 6 min illumination (dash-dotted line). The insets show the region of the >C=O stretching mode around 1721 cm^{-1}.

0935-9648/02/0704-0484 $ 17.50+.50/0

absorption in toluene solution, and more pronounced and bathochromically shifted in the solid state at ca. 2.6–2.8 eV, is identified as the absorbance of the fluorenone chromophores (π–π* transition).[40] This low-energy absorption tail/shoulder is absent in pristine DA-PF both in dilute solution and in the solid state.

The energetic position of the low-energy emission band at ca. 2.3 eV in MA-PF is very similar to the low-energy emission band of the fluorenone building block in statistical dialkylfluorene/fluorenone copolymers.[16,51] It is also similar to the emission band of photooxidized (photodegradated) fluorene-endcapped poly(9,9-dihexylfluorene-2,7-diyl) (PF6) as demonstrated by the IBM Almaden group,[42] where, terminal, unsubstituted fluorene moieties were photooxidized to fluorenone units. These findings strongly support the presented assignment of our experimental results. In this light, the often favored interpretation that the low-energy emission bands in PF (and also in ladder-type poly(*para*-phenylene)s LPPP, in which such low-energy emission bands also occur at a similar spectral position of ca. 2.2 eV!) are associated with ongoing aggregate or excimer formation[38–39] is at the very least questionable.

In contrast, we propose that the keto defects act as "guest" emitters that efficiently trap singlet excitons created on the conjugated PF backbone by a dipole–dipole induced direct excitation energy transfer of the Förster-type[43] or an excitation energy migration (EEM)-assisted Förster-type transfer process.[44,45] This process becomes the dominating channel of excited state depopulation in the solid state. Due to the reduced or inhibited **inter**chain Förster-type (or EEM-assisted Förster-type) energy transfer to the keto defect sites the contribution of the low-energy PL band at ca. 2.3 eV in dilute solutions of MA-PF is only moderate. Moreover, we have performed quantum-chemical simulations to gain a deeper insight into the nature of the electronic states involved in the absorption and emission processes in these materials by coupling the intermediate neglect of differential overlap (INDO) Hamiltonian to a configuration interaction (CI) approach.[46] For MA-PF containing keto defect sites, these calculations show a localization of the emissive excited states on the fluorenone unit prior to recombination, while the emissive excited state is delocalized over several fluorene segments in pristine DA-PF free of keto defect sites. These findings indicate that the exciton localization at the fluorenone sites additionally enhances the emission intensity at ca. 2.3 eV.

The keto defect sites present in MA-PF are formed already during the synthesis of the polymer. However, such keto defect sites can not only be formed as side reaction during polymer synthesis, as shown for MA-PF, but can also be formed as result of a photo- or (electro-)oxidative degradation of DA-PF. In order to demonstrate the degradation-induced creation of keto-defects, DA-PF samples were studied in photooxidation as well as in electrooxidation experiments.

Figure 9 shows the PL spectrum of a pristine DA-PF film and the subsequently degraded layer. Photooxidation of the sample for 6 min yields a dramatic decrease of the integral PL

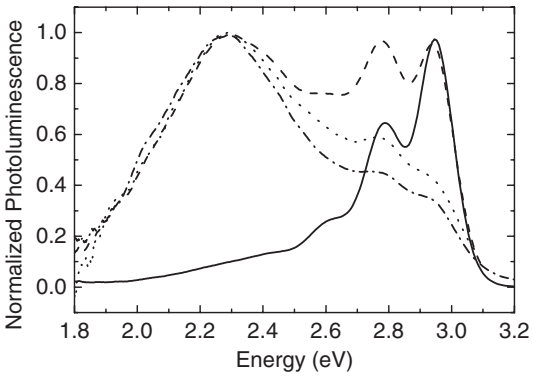

Fig. 9. Photoluminescence emission spectrum of a "pristine" DA-PF film (full line), and after photooxidation (1000 W xenon lamp under air) for 2 (dashed line), 4 (dotted line), and 6 min illumination (dash-dotted line).

quantum yield to approximately 10 % of the initial value. Simultaneously, the low-energy emission band at 2.3 eV emerges and increases relative to the initial PF emission during ongoing photooxidation of DA-PF. Furthermore, in the simultaneously measured IR spectra (depicted in Fig. 8b) one finds the appearance of a fluorenone-related signal (>C=O stretching mode) at 1721 cm^{-1}, which increases gradually. These findings clearly prove the formation of emissive fluorenone defects upon degradation.

Figure 10 depicts the electroluminescence spectrum of an ITO/MA-PF/Al device (OLED, solid line), an ITO/DA-PF/Al device (dashed line), and an ITO/DA-PF/Al device after

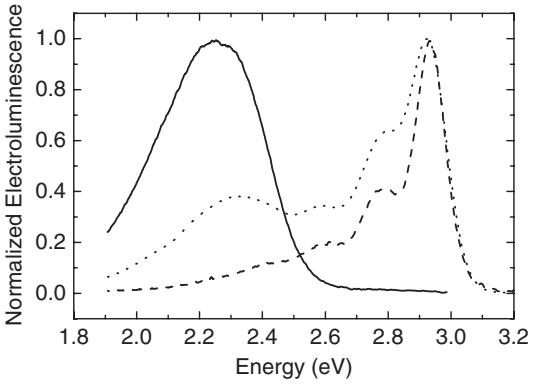

Fig. 10. Electroluminescence spectrum of an ITO/MA-PF/Al device (solid line), an ITO/DA-PF/Al device (dashed line), and the ITO/DA-PF/Al device (dotted line) after 30 min continuous operation under air (electrooxidative degeneration).

30 min of continuous operation at 14 V at a current density of 1 mA cm^{-2} under air. The EL spectrum of the MA-PF-based device is completely dominated by the low-energy emission band at ca. 2.25 eV, which causes a yellow–orange emission, similar to the emission found for a OLED with poly(9-fluorenone) as emissive layer.[47] Remarkably, the emissive contribution of the keto defect sites is more pronounced in EL when compared to the above discussed PL experiments. The reason for this behavior is the presence of two parallel processes that yield the low-energy EL contribution: a) energy transfer of singlet excitons from the PF main chain to keto defect sites and b) trapping of charges at the fluorenone defect

  0935-9648/02/0704-0485 $ 17.50+.50/0

sites and their subsequent emissive recombination with oppositely charged charge carriers. The second process cannot proceed in PL experiments and increases the relative contribution of the defect-site-related low-energy EL band. Therefore, in contrast to the PL process, in EL devices a much lower concentration of fluorenone defects results in a dominating low-energy emission band (studies on related energy-transfer processes have also been published[48,49]).

For the DA-PF-based OLEDs, a stable and efficient blue emission occurs at turn on voltages of ca. 8 V.[50] However, the color changes into a blue–greenish emission after more than 30 min of continuous operation in air without special encapsulation of the OLED device. Note that such atmospheric conditions are usually not applied in OLEDs for long-term applications. The EL spectrum of the "degraded" devices exhibits an additional low-energy emission band at ca. 2.3 eV, which we now also assign to the formation of fluorenone defect sites. This finding demonstrates that the formation of fluorenone defect sites also occurs under operation of OLEDs based on DA-PF, especially under atmospheric conditions.

Our assignment of the 2.3 eV emission band to keto defect sites is also fully in line with very recent investigations on novel fluorene-based copolymers containing a well-defined fraction of 9-fluorenone units.[51] We find that the solid-state emission spectrum of these copolymers (with 0.1, 0.2, 0.5, 1.0, and 2.0 mol- % of fluorenone moieties) displays the above discussed emission band at ca. 2.3 eV of increasing intensity with increasing fluorenone content, both in PL and EL.

Regarding this, our degradation-related results strongly indicate the key role of keto defect sites as the source of the often observed low energy emission bands, most pronounced for polyfluorenes with methylene-bridge hydrogen substituents (as MA-PF). The findings illustrate the superiority of difunctionalization at the methylene group in all -CR_2-bridged polyphenylene and polyarylene derivatives (e.g., polyfluorenes PF, but also ladder-type poly(*para*-phenylene)s, LPPP).

As demonstrated previously, the decoration of the polyfluorene backbone with arylene-type dendronic side-chains also leads to an increased chemical stability and reduced interchain energy transfer.[17] The first finding may, thereby, be related to an increased photooxidative stability of 9,9-diarylated PF derivatives.

6. Conclusion

The photo- or electrooxidative degradation processes that lead to low-energy emission bands also in disubstituted, "hydrogen-free" DA-PF and LPPP derivatives (e.g., PF8, PF2/6, and MeLPPP)[25,52] have to be further studied. This is a very urgent topic especially in order to improve the long-term and color stability of polyarylene-based blue OLEDs. Preliminary results suggest that the photo- (or electro-)oxidative degradation of DA-PFs is probably coupled to the presence of a small (sub-percent) amount of only monoalkylated fluorene building blocks. Therefore, the use of exceptionally pure 9,9-dialkylated dibromofluorene monomers seems to be of primary importance. These findings also explain the often observed batch-to-batch differences in the optical properties (causing a different photooxidative stability) of one and the same PF derivative.

Due to the limited space for this review, we have not discussed the enormous progress towards high-efficiency PF-based OLEDs in the frame of the review article.[9,53,54] This special device-related topic is e.g., outlined in a previously published review by Neher.[55] Recent activities in the fabrication of OLEDs that showed an electroluminescence of high, linear polarization ratios and whose active layers are based on aligned liquid-crystalline PFs have not been considered and included here.[28,55,56]

The herein extensively discussed photophysical topics, 1) structure- and morphology-dependent conformational changes of the PF main chain, and 2) influence of defect sites on the optical and electronic properties, are of key importance for establishing reliable structure–property relationships, and therefore for controlling and fine-tuning the materials properties of PF-type polymers.

Received: January 22, 2002

[1] M. Fukuda, K. Sawada, K. Yoshino, *J. Polym. Sci. A: Polym. Chem.* **1993**, *31*, 2465.
[2] Q. B. Pei, Y. Yang, *J. Am. Chem. Soc.* **1996**, *118*, 7416.
[3] a) E. P. Woo, M. Inbasekaran, W. Shiang, G. R. Roof, *International Patent Application WO 97/05184*, **1997** [*Chem. Abs.* **1997**, *126*, 225 700y]. b) M. T. Bernius, M. Inbasekaran, J. O'Brien, W. S. Wu, *Adv. Mater.* **2000**, *12*, 1737.
[4] M. Ranger, M. Leclerc, *Macromolecules* **1997**, *30*, 7686.
[5] H.-G. Nothofer, A. Meisel, T. Miteva, D. Neher, M. Forster, M. Oda, G. Lieser, D Sainova, A. Yasuda, D. Lupo, W. Knoll, U. Scherf, *Macromol. Symp.* **2000**, *154*, 139.
[6] E. J. W. List, R. Güntner, P. Scandiucci de Freitas, U. Scherf, *Adv. Mater.* **2002**, *14*, 374.
[7] G. Fytas, H.-G. Nothofer, U. Scherf, D. Vlassopoulos, G. Meier, *Macromolecules* **2002,** *35*, 481.
[8] G. Klärner, J.-I. Lee, V. Y. Lee, E. Chan, J.-P. Chen, A. Nelson, D. Markiewicz, R. Siemens, J. C. Scott, R. D. Miller, *Chem. Mater.* **1999**, *11*, 1800.
[9] a) T. Miteva, A. Meisel, W. Knoll, H.-G. Nothofer, U. Scherf, K. Müller, K. Meerholz, A. Yasuda, D. Neher, *Adv. Mater.* **2001**, *13*, 565. b) D. C. Müller, T. Braig, H.-G. Nothofer, M. Arnoldi, M. Gross, U. Scherf, O. Nuyken, K. Meerholz, *ChemPhysChem* **2000**, *1*, 207.
[10] G. Klärner, R. D. Miller, C. J. Hawker, *Polym. Prepr.* **1998**, 1047.
[11] C. Schmitt, H.-G. Nothofer, A. Falcou, U. Scherf, *Macromol. Rapid Commun.* **2001**, *22,* 624.
[12] a) G. Klärner, M. H. Davey, W.-D. Chen, J. C. Scott, R. D. Miller, *Adv. Mater.* **1998**, *10*, 993. b) M. Kreyenschmidt, G. Klärner, T. Fuhrer, J. Ashenhurst, S. Karg, W.-D. Chen, V. Y. Lee, J. C. Scott, R. D. Miller, *Macromolecules* **1998**, *31*, 1099. c) J.-I. Lee, G. Klärner, M. H. Davey, R. D. Miller, *Synth. Met.* **1999**, *102*, 1097. d) U. Asawapirom, U. Scherf, *Macromol. Rapid Commun.* **2001**, *22*, 746. e) C. Xia, R. C. Advincula, *Macromolecules* **2001**, *34*, 5854.
[13] a) M. Redecker, D. D. C. Bradley, M. Inbasekaran, W. Wu, E. Woo, *Adv. Mater.* **1999**, *11*, 241. b) M. Redecker, D. D. C. Bradley, K. Baldwin, D. Smith, M. Inbasekaran, W. Wu, E. Woo, *J. Mater. Chem.* **1999**, *9*, 2151. c) P. Blondin, J. Bouchard, S. Beaupre, M. Belletete, G. Durocher, M. Leclerc, *Macromolecules* **2000**, *33*, 5874. d) B. Liu, W.- L. Yu, Y.-H. Lai, W. Huang, *Macromolecules* **2000**, *33*, 8945.
[14] A. J. Cadby, P. A. Lane, H. Mellor, S. J. Martin, M. Grell, C. Giebeler, D. D. C. Bradley, M. Wohlgenannt, C. An, Z. V. Vardeny, *Phys. Rev. B* **2000**, *62*, 15 604.
[15] M. Grell, D. D. C. Bradley, X. Long, T. Chamberlain, M. Inbasekaran, E. Woo, M. Soliman, *Acta Polym.* **1998**, *49*, 439.
[16] H.-G. Nothofer, *Ph.D. Thesis*, Universität Potsdam, Germany **2001**; Logos Verlag, Berlin, **2001**, ISBN 3-89722-668-5.

  0935-9648/02/0704-0486 $ 17.50+.50/0

[17] S. Setayesh, A. C. Grimsdale, T. Weil, V. Enkelmann, K. Müllen, F. Meghdadi, E. J. W. List, G. Leising, *J. Am. Chem. Soc.* **2001**, *123*, 946.
[18] D. Marsitzky, R. Vestberg, P. Blainey, B. T. Tang, C. J. Hawker, K. F. Carter, *J. Am. Chem. Soc.* **2001**, *123*, 6965.
[19] M. Grell, D. D. C. Bradley, G. Ungar, J. Hill, K. S. Whitehead, *Macromolecules* **1999**, *32*, 5810.
[20] G. Lieser, M. Oda, T. Miteva, A. Meisel, H.-G. Nothofer, U. Scherf, D. Neher, *Macromolecules* **2000**, *33*, 4490.
[21] L. Pu, *Acta Polym.* **1997**, *48*, 116.
[22] J. A. Teetsov, D. A. Vanden Bout, *J. Am. Chem. Soc.* **2001**, *123*, 3605.
[23] M. Grell, D. D. C. Bradley, M. Inbasekaran, E. Woo, *Adv. Mater.* **1997**, *9*, 798.
[24] H. Sirringhaus, R. J. Wilson, R. H. Friend, M. Inbasekaran, W. Wu, E. Woo, M. Grell, D. D. C. Bradley, *Appl. Phys. Lett.* **2000**, *77*, 406.
[25] J. Teetsov, M. A. Fox, *J. Mater. Chem.* **1999**, *9*, 2117.
[26] M. Oda, H.-G. Nothofer, G. Lieser, U. Scherf, S. C. J. Meskers, D. Neher, *Adv. Mater.* **2000**, *12*, 362.
[27] B. Schartel, V. Wachtendorf, M. Grell, D. D. C. Bradley, M. Hennecke, *Phys. Rev. B* **1999**, *60*, 277.
[28] M. Grell, W. Knoll, D. Lupo, A. Meisel, T. Miteva, D. Neher, H.-G. Nothofer, U. Scherf, A. Yasuda, *Adv. Mater.* **1999**, *11*, 671.
[29] D. Sainova, A. Zen, H.-G. Nothofer, U. Asawapirom, U. Scherf, R. Hagen, T. Bieringer, S. Kostromine, D. Neher, *Adv. Funct. Mater.* **2002**, *12*, 49.
[30] M. Pope, C. A. Swenberg, *Electronic Processes in Organic Crystals*, Oxford University Press **1998**.
[31] E. J. W. List, J. Partee, J. Shinar, U. Scherf, K. Müllen, W. Graupner, K. Petritsch, E. Zojer, G. Leising, *Phys. Rev. B* **2000**, *61*, 10 807.
[32] E. J. W. List, C.-H. Kim, A. K. Naik, U. Scherf, G. Leising, W. Graupner, J. Shinar, *Phys. Rev. B* **2001**, *64*, 155 204.
[33] a) D. Hertel, S. Setayesh, H.-G. Nothofer, U. Scherf, K. Müllen, H. Bässler, *Adv. Mater.* **2001**, *13*, 65. b) C. Rothe, R. Güntner, U. Scherf, A. P. Monkman, *J. Chem. Phys.* **2001**, *115*, 9557. c) D. Hertel, H. Bässler, R. Güntner, U. Scherf, *J. Chem. Phys.* **2001**, *115*, 10 007. d) A. P. Monkman, H. D. Burrows, I. Hamblett, S. Navaratnam, U. Scherf, C. Schmitt, *Chem. Phys. Lett.* **2000**, *327*, 111.
[34] S. C. J. Meskers, J. Hübner, M. Oestreich, H. Bässler, *Chem. Phys. Lett.* **2001**, *339*, 223.
[35] V. G. Kozlov, P. E. Burrows, G. Parthasarathy, S. R. Forrest, *Appl. Phys. Lett.* **1999**, *74*, 1057.
[36] a) N. Tessler, D. J. Pinner, V. Cleave, P. K. H. Ho, R. H. Friend, G. Yahioglu, P. Le Barny, J. Gray, M. de Souza, G. Rumbles, *Synth. Met.* **2000**, *115*, 57. b) U. Scherf, S. Riechel, U. Lemmer, R. Mahrt, *Curr. Opin. Solid State Mater. Sci.* **2001**, *5*, 143.
[37] A. J. Campbell, D. D. C. Bradley, H. Antoniadis, *Appl. Phys. Lett.* **2001**, *79*, 2133.
[38] a) U. Lemmer, S. Heun, R. F. Mahrt, U. Scherf, M. Hopmeier, U. Siegner, E. O. Göbel, K. Müllen, H. Bässler, *Chem. Phys. Lett.* **1995**, *240*, 373. b) V. Cimrová, U. Scherf, D. Neher, *Appl. Phys. Lett.* **1996**, *69*, 608.
[39] a) E. Conwell, *Trends Polym. Sci.* **1997**, *5*, 218. b) M. Grell, D. D. C. Bradley, G. Ungar, J. Hill, K. S. Whitehead, *Macromolecules* **1999**, *32*, 5810.
[40] A. R. G. Ilharco, J. Lopes da Silva, M. João Lemos, L. F. Vieira Ferreira, *Langmuir* **1997**, *13*, 3787.
[41] R. M. Silverstein, G. C. Bassler, T. C. Morrill, *Spectroscopic Identification of Organic Compounds,* 4th ed., Wiley, New York **1981**.
[42] a) V. N. Bliznyuk, S. Carter, J. C. Scott, G. Klärner, R. D. Miller, D. C. Miller, *Macromolecules* **1999**, *32*, 361. b) J. I. Lee, G. Klärner, R. D. Miller, *Chem. Mater.* **1999**, *11*, 1083.
[43] T. Förster, *Ann. Phys.* **1948**, *2*, 55.
[44] E. J. W. List, C. Creely, G. Leising, N. Schulte, A. D. Schlüter, U. Scherf, K. Müllen, W. Graupner, *Chem. Phys. Lett.* **2000**, *325*, 132.
[45] A. R. Buckley, M. D. Rahn, J. H. Hill, J. Cabanillas-Gonzalez, M. A. Fox, D. D. C. Bradley, *Chem. Phys. Lett.* **2001**, *339*, 331.
[46] A. Pogantsch, E. Zojer, J. L. Bredas, R. Guentner, P. Scandiucci de Freitas, U. Scherf, E. J. W. List, unpublished results.
[47] F. Uckert, Y.-H. Tak, K. Müllen, H. Bässler, *Adv Mater.* **2000**, *12*, 905.
[48] E. J. W. List, G. Leising, N. Schulte, A.-D. Schlüter, U. Scherf, W. Graupner, *Jpn. J. Appl. Phys.* **2000**, *39*, L760.
[49] S. Tasch, E. J. W. List, C. Hochfilzer, G. Leising, P. Schlichting, U. Rohr, Y. Geerts, U. Scherf, K. Müllen, *Phys. Rev. B* **1997**, *56*, 4479.
[50] The elevated turn on voltages of the presented OLEDs is due to the use of a high work function metal (Al) as top metal electrode, which has been chosen to avoid possible influences of a metal–polymer interface reaction.
[51] P. Scandiucci de Freitas, U. Scherf, M. Collon, E. J. W. List, *e-polymers* **2002**, in press.
[52] W. Graupner, J. Partee, J. Shinar, G. Leising, U. Scherf, *Phys. Rev. Lett.* **1996**, *77*, 2033.
[53] M. Gross, D. Müller, H.-G. Nothofer, U. Scherf, D. Neher, C. Bräuchle, K. Meerholz, *Nature* **2000**, *405*, 661.
[54] a) K. H. Weinfurtner, H. Fujikawa, S. Tokito, Y. Taga, *Appl. Phys. Lett.* **2000**, *76*, 2502. b) T. Virgili, D. G. Lidzey, D. D. C. Bradley, *Adv Mater.* **2000**, *12*, 58. c) R. W. T. Higgins, H.-G. Nothofer, U. Scherf, A. P. Monkman, *Appl. Phys. Lett.* **2001**, *79*, 857. d) R. W. T. Higgins, H.-G. Nothofer, U. Scherf, A. P. Monkman, *J. Appl. Phys.* **2002**, *91*, 99.
[55] D. Neher, *Macromol. Rapid Commun.* **2001**, *22*, 1365.
[56] K. S. Whitehead, M. Grell, D. D. C. Bradley, M. Jandke, P. Strohriegl, *Appl. Phys. Lett.* **2000**, *76*, 2946.

  0935-9648/02/0704-0487 $ 17.50+.50/0